LA-UR- 98-1249

Approved for public release; distribution is unlimited.

Title: NUMERICAL SIMULATION OF IN SITU BIOREMEDIATION

CONF-980670--

Author(s): BRYAN J. TRAVIS, EES-5

Submitted to: XII INTERNATIONAL CONFERENCE ON COMPUTATIONAL METHODS IN WATER RESOURCES, CRETE, GREECE, JUNE 15-19, 1998

DISTRIBUTION OF THIS DOCUMENT IS UNLIMITED

MASTER

Los Alamos
NATIONAL LABORATORY

DISCLAIMER

Numerical Simulation of In Situ Bioremediation

Bryan J. Travis

Earth and Environmental Sciences Division, Los Alamos National Laboratory, Los Alamos, NM 87545; EMail: bjt@vega.lanl.gov

Abstract

Models that couple subsurface flow and transport with microbial processes are an important tool for assessing the effectiveness of bioremediation in field applications. A numerical code is described that differs from previous in situ bioremediation models in that it includes: both vadose and groundwater zones, unsteady air and water flow, limited nutrients and airborne nutrients, toxicity, co-metabolic kinetics, kinetic sorption, subgridscale averaging, pore clogging and protozoan grazing.

Introduction

Organic materials such as chlorinated solvents and petroleum products are among the most common contaminants of ground water and soils. In recent years, several alternative environmental restoration technologies have been compared for their effectiveness at removing such contaminants. One of the more promising is *in situ* bioremediation, the use of microbes to convert hazardous chemicals to environmentally benign products such as water, carbon dioxide, biomass, and salts.

Numerical modeling of bioremediation has been a useful adjunct to design of in situ bioremediation operations. Models are valuable because they provide a mechanism for combining the various kinds of data we have on a site, from hydrologic and geologic data to microbiological information. Consistency of data, the interactions between processes, sensitivity analysis, interpretation of data, parameter estimation and field operation design are all common uses of models. Further, a calibrated model can provide estimates of the temporal and spatial distribution of concentrations, pressures and saturations everywhere in the subsurface region.

Previous Models

Over the past decade, a number of researchers have published descriptions of in situ bioremediation models. Only a few representative ones are discussed here because of limited space.

The basis of each model has been a set of coupled advection-diffusion-reaction-of-Monod-form (ADRM) equations. Most models considered an electron acceptor (e.g., oxygen), an electron donor (growth substrate) and microbial biomass, in a steady groundwater system (see e.g., Molz, Widdowson and Benefield [1]). Virtually all used an operator-splitting approach, separating transport from reactions, with iteration (full or limited) to reconcile the split operators. Solution methods included reduction to a set of stiff ordinary differential equations solved with an adaptive time step algorithm (Borden & Bedient [2]), a fully upwinded finite difference, iterative Newton-Raphson-Kantorovich algorithm (Widdowson, Molz and Benefield [3]), optimal test functions involving computation of the adjoint equations (Celia, Kindred and Herrera [4]), principal direction Galerkin finite elements (MacQuarrie, Sudicky and Frind [5]), Runge-Kutta integration for the reactive terms (Rifai, and Bedient [6]), and characteristic finite elements (Wheeler, Roberson & Chilakapati [7]).

Some models have focused on extension of the physical and biochemical processes. For example, Semprini and McCarty [8] added co-metabolism and competitive inhibition for TCE degradation. Schafer and Kinzelbach [9] investigated the impact of soil heterogeneity on bioremediation efficiency in a 2-D system for facultative anaerobe microbes. Wheeler, Roberson & Chilakapati [7] also studied bioremediation in 3-D, heterogeneous soils. Nicol, Wise, Molz, and Benefield [10] considered multiple microbial species. Zysset, Stauffer, and Dracos [11] emphasized the dynamics of biofilms in their model. Essaid, Bekins, Godsy, Warren, Baedecker and Cozzarelli [12] focussed on the different degradative zones that arise during multispecies reactive solute transport with sequential aerobic and anaerobic processes in 2-D flow fields.

TRAMPP Model

Previous models have focused almost exclusively on steady saturated flow with water-borne delivery of nutrients or with nutrients in excess. The TRAMPP model of Travis and Rosenberg [13] included both the vadose and groundwater zones, unsteady air and water flow, with limited nutrients and airborne delivery of nutrients in their application of the TRAMPP ADRM model to the Savannah River site. In addition their model includes toxicity of byproducts to microbes, multiple substrates and nutrients, competitive inhibition, co-metabolic kinetics, rate-limited sorption, pore clogging and permeability changes, and multiple microbial species and predator grazing.

TRAMPP contains two sets of equations. The first set includes the flow equations for unsaturated/saturated flow of air and water in heterogeneous media in 1-, 2- or 3-D geometries. Material properties, such as porosity and permeability, can vary in space and time. The model allows several boundary condition types, and injection/ extraction wells. Conservation of mass for the air phase is

$$\frac{\partial(\varepsilon\rho_g f)}{\partial t} + \nabla\cdot\left(\rho_g\vec{u}_g\right) = \varepsilon\dot{S}_g \tag{1}$$

and for the water (liquid + vapor) phase is

$$\frac{\partial(\varepsilon(\rho_W\sigma + f\rho_V))}{\partial t} + \nabla\cdot\left(\rho_W\vec{u}_W + \rho_V\vec{u}_g\right) = \varepsilon\dot{S}_W \tag{2}$$

The momenta conservation equations are approximated by Darcy's law (for low Reynolds number flows):

$$\vec{u}_i = -\frac{k_i}{\mu_i}\left(\nabla P_i + \rho_i\hat{g}\right),\ k_i = k_i(\sigma, C_M),$$
$$P_g - P_w = P_c(\sigma),\ \rho_v = \rho_v(T,\sigma) \tag{3}$$

where the subscript i refers to the phase, P is pressure, T is temperature, Pc is capillary pressure, u is velocity, k is permeability (scalar, vector, or tensor), ε is porosity, f is air saturation, σ is water saturation, ρ is density, subscripts g, v and w refer to gas, vapor and water phases, t is time, $\dot{S}$ is a source/sink term, and μ is viscosity. The permeability k is a function of saturation and total microbial concentration C_M. Pore clogging occurs at moderate to high C_M values (Jennings et al. [14]). At present, a simple linear dependence of k on C_M between a lower and an upper saturation value is used.

The permeability k at many sites has structure over many scales. In a numerical solution, a lower size limit is imposed implicitly through the size of discretization elements. Subgridscale structure is lost unless special efforts are made to capture it, e.g., through homogenization, renormalization, stochastic analysis, or other means. In this model, subgridscale structure can be captured through "fractal homogenization". Homogenization of a region replaces the fine scale permeability with a tensor that yields roughly the same flux through the sides of the region as would occur in the finely zoned case. With fractal scaling, the porous medium is assumed to be fractal in its distribution of properties. Using fractal interpolating functions (Barnsley [15]), the subgridscale region can be integrated directly to provide an equivalent gridscale value. Under certain circumstances, the fractal representation can be used to integrate the reactive system equations and obtain a solution valid at all scales.

The form of the transport equations in conservative form is:

$$L_i(C_i) = \frac{\partial[\varepsilon C_i(\sigma\rho_w + fH^i) + (1-\varepsilon)\rho_s C_{is}]}{\partial t} + \nabla \cdot \left((\overrightarrow{u_w} + H^i \overrightarrow{u_g})C_i\right) - \nabla \cdot \left[\varepsilon(\sigma D_w{}^i + f H^i D_g{}^i) \nabla C_i\right] - \varepsilon\sigma\rho_w B_R^i(C_1, C_2, \ldots) = 0 \quad (4)$$

where C_i is aqueous concentration of species i, s refers to sorbed phase, D is diffusivity/dispersivity, H is Henry's Law coefficient, and B^i_R represents the various metabolic and microbial interactions (see Travis & Rosenberg [13] for details). Number of species is arbitrary.

Sorption/desorption into/out of soil grains can take tens of days; it is represented by:

$$\frac{dC_{is}}{dt} = \frac{(K_d^i C_i - C_{is})}{\tau^i} \quad (5)$$

where K_d is the equilibrium sorption coefficient, and τ is the time scale for solid phase diffusion and is a function of soil particle radius. Protozoa are typically mobile. However, microbes tend to form films on soil grains, with slow rate of detachment. Details of biofilm structure are ignored here.

Numerical Algorithm

The numerical approach taken here is to use integrated (mass-conservative) finite difference approximations to the governing equations, treat nonlinearities in an iterative fashion and use residual reduction as the convergence criterion, resulting in very small mass balance errors. Transport and catabolic reaction terms are separated through operator-splitting, but are made self-consistent through (Newton-Raphson) iteration. The components of the model have been tested successfully against analytical solutions and experimental results for a variety of flow, transport and reaction conditions.

The flow eqs 1-3 are solved simultaneously through a coupled, Newton-Raphson iteration on the residual formulation of the difference equations. This allows highly variable saturation conditions, including almost dry conditions, to be simulated. Transport equations are solved separately from the flow. However, if permeability changes due to pore clogging are large during a time step, a second, "corrector" pass on the flow equations is carried out.

Separation of transport processes from reaction processes is the basis for the iterative solution technique. We divide the operator L into two operators:

$$\bar{L}_i = \bar{L}_i^{tr} + \bar{L}_i^{rx} \tag{6}$$

The two operators are defined as:

$$\left(\bar{L}_i^{tr}\right)^k = A_i^{n+1}C_i^k - A_i^nC_i^n + \frac{\Delta t}{\Delta\Omega}\sum_{j=1}^{6}(\vec{u_w} + H^i\vec{u_g})_j(C_ij)^k\Delta a_j$$

$$- \sum_{j=1}^{6}\varepsilon(\sigma D^i_w + f\,H^iD^i_g)_j\frac{\Delta a_j}{\Delta x_j}\left[(C_ij)^k - (C_i)^k\right]$$

$$- \frac{\varepsilon\sigma}{2}\rho_w(B_R^{i,n} + B_R^{i,k-1})\Delta t \tag{7}$$

and

$$\left(\bar{L}_i^{rx}\right)^k = A_i^{n+1}C_i^{n+1} - A_i^{n+1}C_i^k$$

$$- \frac{\varepsilon\sigma}{2}\rho_w(B_R^{i,n+1} - B_R^{i,k-1})\Delta t \tag{8}$$

where $A_i = \varepsilon\sigma + \varepsilon\, f\, H^i + (1-\varepsilon)\,\rho_s\, K_d{}^i\, R^i$, $t^{n+1} = t^n + \Delta t$, (9)

Δt is the current value of the time step, the superscript 'k' refers to an intermediate value between time levels n and n+1, Δa_j is the area of the j-th face of a grid cell, $\Delta\Omega$ is a grid cell volume, Δx_j is the distance between cell centers on the j-th side of each grid cell, and Σ represents summation over the faces of a grid cell. Since terms $B_R^{i,n+1}$ are nonlinear, we expand in a Taylor series to first order around C_i^k. Eqs 8 become:

$$\left(\bar{L}_i^{rx}\right)^k \approx A_i^{n+1}C_i^{n+1} - A_i^{n+1}C_i^k - \frac{\varepsilon\sigma}{2}\rho_w\Delta t\,(B_R^{i,k} - B_R^{i,k-1}$$

$$+ \sum_{m=1}^{N_c}\frac{\partial B_R^{i,k}}{\partial C_m}(C_m^{n+1} - C_m^k)) \tag{10}$$

The iterative solution of eqs 7 and 10 is accomplished in the following manner. From knowledge of the values of C_i^n and C_i^{k-1}, eqs 7 are solved implicitly for the C_i^k. This step emphasizes the transport processes. In eq 7, $B_R^{i,k-1}$ is evaluated using C_i^{k-1} values. (On the first iteration of a time step $C_i^{k-1} = C_i^n$). Next, eqs 10 are

solved for the C_i^{n+1}. This step emphasizes the reactions between species. Since each B_R^i depends on the concentrations of all N_c species, a set of N_c simultaneous equations are solved in each grid cell. Newton-Raphson iteration of eqs 10 converges very rapidly to small tolerances (typically 10^{-12} to 10^{-16}). When eqs 10 have converged in each cell, eqs 7 are solved again, using the results of the last solution of eqs 10 to evaluate the $B_R^{i,k-1}$ terms. This process is repeated until convergence on eqs 7 occurs.

Mass balance errors over an entire simulation involving strongly nonlinear behavior usually remain less than 1% and frequently much less than 1%. Mass balance for the flow equations is generally accurate to one part in 10^6 or better.

Discussion

One of the major shortcomings in previous models of in situ bioremediation which limit their predictive power is inadequate treatment of microbial community interactions. In a natural setting, soil bacteria live in a community of organisms, including other bacterial species, fungi, and various protozoa. A particular species that will readily degrade a contaminant in the laboratory may have to compete for growth substrates and nutrients and may suffer predation in the natural setting, reducing its degradative efficiency.

An example of how microbial interactions can affect in situ bioremediation is clearly illustrated in the following example. In this simple 1-D geometry, a hydrocarbon contaminant plume is moving from left to right with groundwater through a region at a fixed velocity of 0.8 ft/day. The groundwater contains dissolved oxygen and nutrients. A bacterial species is present in the soil which will grow on the hydrocarbon substrate. There is also a common soil protozoan species that will consume the bacterial species. Protozoan grazing of contaminant-eating bacteria has been observed (Sinclair [16]). Protozoan grazing has been found to follow Monod kinetics. In isolation, the indigenous bacteria would be able to consume the invading contaminant plume rapidly. The presence of a predatory protozoan species complicates this. Figure 1 shows simulated bacterial and protozoan concentrations and the substrate concentration as a function of position and time. The time window is between 200 and 300 days after first arrival of the plume at X=0. Interesting nonlinear behavior arises due to microbial species interactions which are not seen when only one species is considered. The bacterial and protozoan species experience episodic growth and decay. The oscillations are very regular in the first meter, then undergo a period doubling and become less regular where the substrate is greatly diminished. A range of other behavior is possible for various combinations of species and will be explored in future computational and experimental studies.

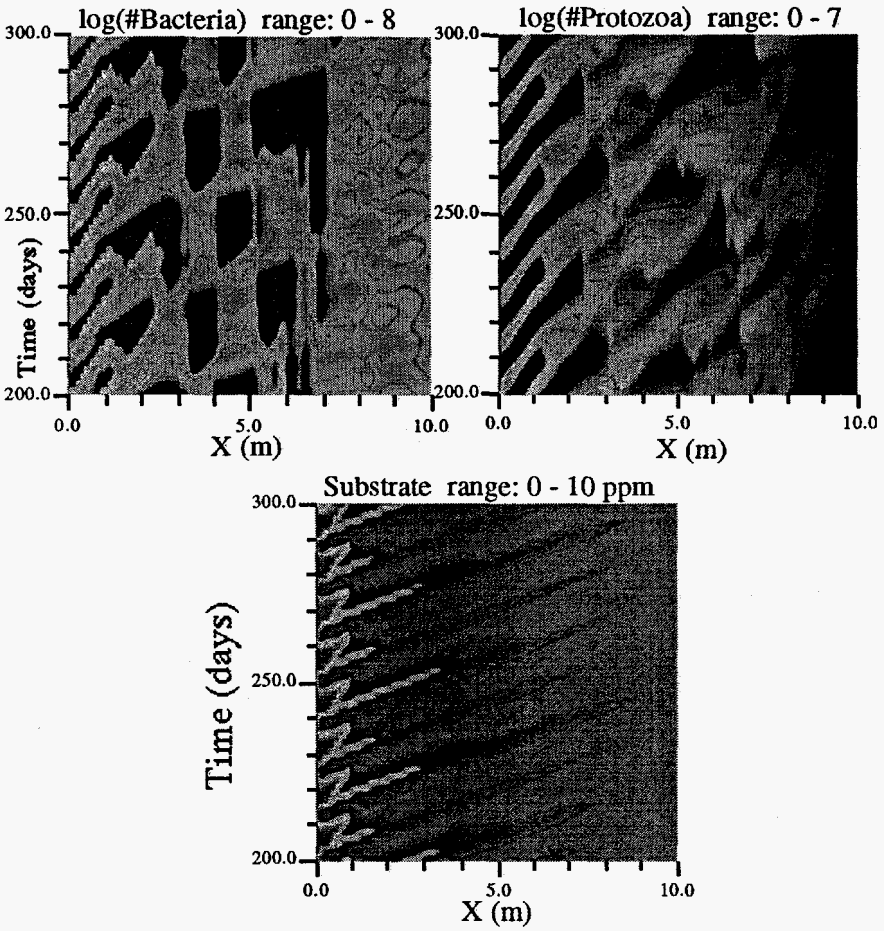

Figure 1. Banded gray scale shading of bacterial and protozoan dynamics. Flow is from left to right at 1 cm/hr, and substrate concentration at X=0 is constant 10 ppm.

References

[1] Molz, F. J., Widdowson, M.A., and Benefield, L.D., Simulation of Microbial Growth Dynamics Coupled to Nutrient and Oxygen Transport in Porous Media, *WRR*, **22**(8), 1207-1216, 1986.

[2] Borden, R. C., and Bedient, P.B., Transport of Dissolved Hydrocarbons Influenced by Oxygen-Limited Biodegradation 1. Theoretical Development, *WRR*, **22**(13), 1973-1982, 1986.

[3] Widdowson, M. A., Molz, F.J., and Benefield, L.D., A Numerical Transport Model for Oxygen- and Nitrate-Based Respiration Linked to Substrate and Nutrient Availability in Porous Media, *WRR*, **24**(9), 1553-1565, 1988.

[4] Celia, M. A., Kindred, J. S., and Herrera, I., Contaminant Transport and Biodegradation 1. A Numerical Model for Reactive Transport in Porous Media, *WRR*, **25**(6), 1141-1148, 1989.

[5] MacQuarrie, K. T. B., Sudicky, E. A., and Frind, E. O., Simulation of Biodegradable Organic Contaminants in Groundwater 1. Numerical Formulation in Principal Directions, *WRR*, **26**(2), 207-222, 1990.

[6] Rifai, H. S., and Bedient, P. B., Comparison of Biodegradation Kinetics With an Instantaneous Reaction Model for Groundwater, *WRR*, **26**(4), 637-645, 1990.

[7] Wheeler, M.F., Roberson, K.R., and Chilakapati, A., Three-dimensional bioremediation modeling in heterogeneous porous media, *Computational Methods in Water Resources IX* vol. 2, eds: T.F. Russell, R.E. Ewing, C.A. Brebbia, W.G. Gray and G.F. Pinder, Boston, 1992.

[8] Semprini, L., and McCarty, P. L., Comparison Between Model Simulations and Field Results for In-Situ Biorestoration of Chlorinated Aliphatics: Part 2. Cometabolic Transformations, *Groundwater*, **30**(1), 37-44, 1992.

[9] Schafer, W., and Kinzelbach, W., Stochastic modeling of in situ bioremediation in heterogeneous aquifers, *J. Contam. Hydro.*, **10**, 47-73, 1992.

[10] Nicol, J.-P., Wise, W. R., Molz, F. J., and Benefield, L. D., Modeling biodegradation of residual petroleum in a saturated porous column, *WRR*, **30**, 3313-3325, 1994.

[11] Zysset, A., Stauffer, F., and Dracos, T., Modeling of reactive groundwater transport governed by biodegradation, *WRR*, **30**(8), 2423-2434, 1994.

[12] Essaid, H.I., Bekins, B.A., Godsy, E.M., Warren, E., Baedecker, M.J., and Cozzarelli, I.M., Simulation of aerobic and anaerobic biodegradation processes at a crude oil spill site, *WRR* **31**(12), 3309-3327, 1995.

[13] Travis, B. J., and Rosenberg, N. D., Modeling *In Situ* Bioremediation of TCE at Savannah River: Effects of Product Toxicity and Microbial Interactions on TCE Degradation, *Environ. Sci. & Tech*, **31**(11), 3093-3102, 1997.

[14] Jennings, D. A., J. N. Petersen, R. S. Skeen, B. M. Peyton, B. S. Hooker, D. L. Johnstone, and D. R. Yonge, An experimental study of microbial transport in porous media,, *Bioaugmentation for Site Remediation*, eds. R. E. Hinchee et al., Battelle Press, Columbus OH, pp. 97-103, 1995.

[15] Barnsley, M. F., *Fractals Everywhere*, Academic Press, Orlando, 1988.

[16] Sinclair, J.L., D.H. Kampbell, M.L. Cook and J.T. Wilson. Protozoa in Subsurface Sediments from Sites Contaminated with Aviation Gasoline or Jet Fuel, *Applied & Eviron. Microbiology*, 59, 467-472, 1993.